Time-lapse full-waveform inversion by model order reduction using radial basis function

Haipeng Li and Robert G. Clapp, Stanford University*

SUMMARY

This study investigates model order reduction (MOR) in time-lapse full-waveform inversion (FWI) using radial basis function (RBF). It introduces a dual-parameterization approach that combines a reduced-order basis space for time-lapse changes with a finite-difference (FD) grid for the baseline model, facilitating wave propagation. The RBF approach allows for representing time-lapse changes on a nonuniform grid, offering variable resolution. This method is validated through three synthetic examples: a CO_2 plume monitoring scenario, a reflection-based time-lapse FWI, and an extension to elastic FWI for near-surface monitoring using surface waves. Results demonstrate effective MOR without compromising FWI accuracy, provide implicit regularization for various geological structures, and highlight the method's potential to enhance computational efficiency in advanced inversion techniques such as Newton-like methods and Hamiltonian Monte Carlo for Bayesian inference.

INTRODUCTION

Time-lapse seismic monitoring is an important method for detecting and characterizing subsurface changes (Lumley, 2001). Time-lapse full-waveform inversion (FWI) has been proven effective in characterizing subsurface changes at high resolution associated with hydrocarbon production (Hicks et al., 2016) and CO_2 injection (Egorov et al., 2017). Nonetheless, FWI is a high-dimensional inverse problem (Virieux & Operto, 2009). Optimization schemes such as Newton-like methods (Pratt et al., 1998) or the Hamiltonian Monte Carlo method for the Bayesian inference (Gebraad et al., 1998) quickly become intractable with the sharp increase in model dimensionality. Therefore, enhancing the convergence rate or sampling efficiency by reducing the number of model parameters in FWI is essential.

The spatial sampling grid in numerical wave propagation is determined by the stability and numerical dispersion conditions of a chosen numerical scheme. Typically, the size of this spatial sampling grid exceeds the resolution at which seismic data can resolve subsurface geological structures. While uniform down-sampling is a strategy to consider (Cox and Verschuur, 2001), it reduces resolution uniformly, which may not be desirable in time-lapse inversion. Other schemes for the sparse representation of the model space in FWI include image-guided interpolation (Ma et al., 2012) and B-spline interpolation (Barnier et al., 2019). In time-lapse FWI, practitioners desire a down-sampling approach that adapts spatial resolutions, i.e., denser in areas of high interest such as reservoirs and sparser in the overburden areas.

In this study, we investigate the use of RBF for achieving MOR in time-lapse FWI. RBF can represent the model using fewer parameters while maintaining variable spatial resolution (Kadu et al., 2016; Chen et al., 2020; Dahlke et al., 2020). Specifically, our focus is on using RBF to reparameterize the time-lapse changes that are the target of inversion. In the following sections, we first outline our methodology and then demonstrate its application through three different synthetic examples. These tests demonstrate that the proposed method not only effectively reduces the model parameters but also introduces implicit regularization.

METHODOLGY

In FWI, one aims to iteratively update the subsurface parameters using the optimization method to fit the observed seismic waveforms with the synthetic data calculated from the wave equation, given certain prior information. The FWI problem using the L2 norm can be defined as follows:

$$\phi(\mathbf{m}) = \frac{1}{2}||\mathbf{d}^{\text{obs}} - \mathbf{d}^{\text{syn}}||_2^2, \tag{1}$$

where $\mathbf{m}$ denotes the subsurface parameters for inversion, $\mathbf{d}^{\text{obs}}$ denotes the observed waveform data, and $\mathbf{d}^{\text{syn}} = \mathbf{L}(\mathbf{m})$ denotes the synthetic data modelled by the wave equation $\mathbf{L}(\mathbf{m})$. In time-lapse FWI, the objective is to track subsurface changes by inverting seismic data acquired from sequential seismic surveys. Several time-lapse inversion strategies have been proposed. In this study, we adopt the double-difference (DD) approach as proposed by Watanabe et al. (2004) and Zhang & Huang (2013). In this method, the *composite* data are inverted in the monitor FWI, which is defined as follows:

$$\phi(\mathbf{m}_{\text{ml}}) = \frac{1}{2}||\mathbf{d}^{\text{com}} - \mathbf{d}_{\text{ml}}^{\text{syn}}||_2^2, \tag{2}$$

where the *composite* data is defined as $\mathbf{d}^{\text{com}} = \mathbf{d}_{\text{ml}}^{\text{obs}} - \mathbf{d}_{\text{bl}}^{\text{obs}} + \mathbf{d}_{\text{bl}}^{\text{syn}}$.

We introduce a reparameterization method using RBF for targeted changes, while the baseline model remains represented on finite-difference grids. The model space defined in Equation 2 is reformulated as follows:

$$\mathbf{m}_{\text{ml}} = \mathbf{m}_{\text{bl}} + \mathbf{m}_{\text{rbf}}, \tag{3}$$

where $\mathbf{m}_{\text{bl}}$ denotes the baseline model, and $\mathbf{m}_{\text{rbf}}$ denotes RBF-represented reduced-order model space for time-lapse

changes, respectively. The RBF parameterization is further defined by:

$$\mathbf{m}_{\text{rbf}}(\boldsymbol{\lambda};\mathbf{x}) = \sum_{i=1}^{N} \lambda_i \Phi(\|\mathbf{x} - \mathbf{c}_i\|), \tag{4}$$

where N is the number of control points, λ_i denotes the weights associated with the RBF centers $\mathbf{c}_i$, and Φ denotes the selected RBF, respectively. In this study, we employ the Gaussian kernel for the RBF, which is given by $\phi(r) = e^{-\epsilon r^2}$. It is noted here that the sharpness parameter ϵ of the RBF, which controls the kernel's taper, is fixed during inversion due to stability concerns. Its value is empirically determined to match the desired resolution.

With the proposed dual-parameterization strategy, the newly defined sparse model space for time-lapse FWI becomes $\boldsymbol{\lambda}$. The gradient of the misfit function with respect to the new model parameters can be calculated using the chain rule as follows:

$$\frac{\partial \phi}{\partial \boldsymbol{\lambda}} = \frac{\partial \phi}{\partial \mathbf{m}_{\text{ml}}} \frac{\partial \mathbf{m}_{\text{rbf}}}{\partial \boldsymbol{\lambda}}. \tag{5}$$

To achieve adaptive resolution, one can design the RBF centers according to a *priori* density maps. For example, positions of the RBF centers can be more densely arranged in reservoir areas to capture any high-resolution changes, while fewer centers are sufficient for overburden that may experience long-wavelength changes.

For implementation, we leverage the meshing tools in finite element methods to facilitate this strategic placement of RBF centers. Also, we recommend testing a chosen RBF scheme in representing target 4D models before actual inversion to optimize RBF center placement and to select the appropriate parameter ϵ for the RBF. It is helpful to understand the additional errors introduced by the RBF operator. Furthermore, after some preliminary inversions, adaptively repositioning some centers towards regions with significant changes or where the inversion shows high uncertainty can also be considered. As for the computational cost, the computational demand for the proposed RBF operator is marginal, and this operator can be performed on the fly or through pre-computed values as demonstrated in Dahlke (2019).

NUMERICAL EXAMPLES

In this section, we present synthetic examples to demonstrate the effectiveness of our proposed method in three different settings. The first two cases are based on acoustic time-lapse FWI for monitoring CO_2 plume and monitoring oil reservoir, respectively. The third example involves near-surface characterization using surface-wave elastic FWI. For the numerical implementation, we use the staggered grid finite-difference method (Virieux, 1986) to solve the first-order acoustic or elastic wave equation in the velocity-stress formulation, with free-surface conditions at the top and convolutional perfectly matched layer absorbing boundary conditions at the remaining boundaries (Komatitsch & Martin, 2007). The adjoint-state method is used to compute the gradient of the objective function with respect to the model parameters (Plessix, 2006). We solve the inverse problem using the L-BFGS optimizer, which employs the L2-norm misfit function. In the time-lapse FWI, the RBF coefficients are initialized as zeros.

CO_2 plume monitoring with sparse data

Our first synthetic test is based on a realistic CO_2 monitoring model. We repurpose the time-lapse reservoir model from SEG Advanced Modeling (SEAM), which features realistic stratigraphy and structural geology, to mimic CO_2 injection into a depleted reservoir. We first employ the multiphase flow modeling to simulate the injection of a CO2-brine mixture, using the open-source code GEOS (Settgast et al., 2017). We further use rock physics modeling to update the subsurface parameters, where fluid properties are modeled according to Batzle & Wang (1992) for brine and CO2, and fluid inclusion modeling is performed using the Kuster-Toksöz method (Kuster & Toksöz, 1974). Figure 1a displays a selected 2D section of the baseline P-wave velocity model from the entire 3D SEAM model, while Figure 1b illustrates the updates to this model resulting from CO2 injection.

We begin our acoustic FWI with the initial model shown in Figure 1c to build the baseline FWI model, using 12 sources (red stars) with 25 Hz Ricker wavelets and dense receivers (spaced 4 m apart, black triangles). For the monitoring FWI, a sparser but more cost-effective survey is considered, with 3 sources and 100-m spacing surface receivers, as shown in Figure 1e. Figure 1d shows the center positions of RBF to represent the time-lapse unknowns, given the prior of the CO_2 injection area. Dense RBF centers with an average distance of 16 m are placed in the targeted area, whereas sparser RBF centers with an average distance of 100 m are used elsewhere. Figure 1e shows the time-lapse FWI result based on the conventional FD parameterization scheme with a grid size of 8 m, and Figure 1f shows the result using the proposed dual-parameterization strategy. We find that the proposed method can yield a result comparable to the one from the conventional method while achieving a MOR of ~29. It is noted that the result in Figure 1e contains some high-frequency artifacts that may be attributed to the inaccuracy of the baseline FWI model. The result in Figure 1f is smoother as the RBF can impose some smoothness. Still, we notice that the high-wavenumber structures at two sides of the CO_2 plume is less well recovered in the RBF result shown in Figure 1f.

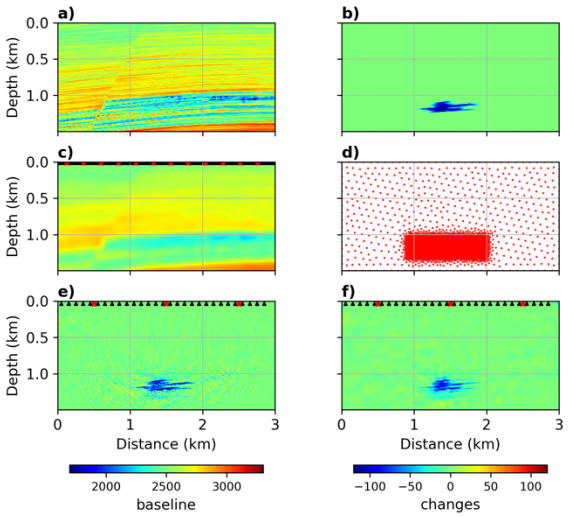

Figure 1: Acoustic time-lapse FWI for CO_2 plume monitoring with sparse data. (a) The baseline P-wave velocity model before CO_2 injection. (b) The P-wave velocity model update reflecting CO2 injection, derived from multiphase flow and rock physics modeling. (c) The initial velocity model for baseline FWI using a survey configuration with 12 sources (red stars) and densely spaced receivers (black triangles, 4 m apart). (d) The positions of RBF centers for reparameterizing the time-lapse changes. (e) Inverted time-lapse changes using conventional FD parameterization. (f) Results employing the proposed RBF reparameterization approach. Note: A sparse survey configuration (3 sources and receivers spaced 100 m apart) is used for monitoring.

Oil reservoir monitoring with reflection data

In the second case, we test our method on a FWI problem using reflection data, aiming to highlight how the RBF reparameterization deals with changes in both reservoir and overburden. Figure 2a shows the baseline P-wave velocity model, which is selected from the SEAM model. Figure 2b shows the time-lapse changes with two anomalies, a short-wavelength velocity perturbation in the reservoir (+100 m/s) and a long-wavelength change peaking at -50 m/s in the overburden. Figure 2c presents the initial model used for the baseline FWI. A narrow-offset survey is considered here to test the reflection FWI, with a total of 11 sources (16 Hz Ricker wavelet) and 10-m spacing receivers. Figure 2d shows the positions of RBF centers, where the reservoir area has dense centers with an average distance of 15 m while the overburden has sparser centers (55 m).

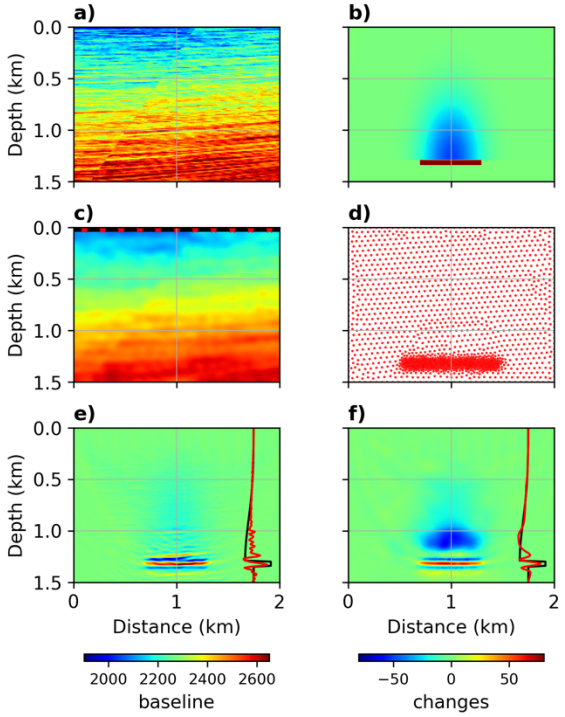

Figure 2: Acoustic time-lapse FWI using the proposed method for oil reservoir monitoring with reflection data. (a) The baseline P-wave velocity model. (b) The true model perturbations representing the time-lapse changes in the reservoir and overburden. (c) The initial velocity model for baseline FWI, with an illustration of sources and receivers. (d) Strategically positioned RBF centers for reparameterizing the time-lapse changes. (e) Inverted time-lapse changes using conventional FD parameterization. (f) Inverted time-lapse changes using the proposed RBF reparameterization approach.

Figure 2e shows the inverted velocity changes using the conventional FD parameterization scheme. In this result, it is observed that the long-wavelength velocity changes are not revealed by the reflection data. These negative blocky changes in the model are erroneously explained by reflector shifts in FWI. This is likely due to the inaccuracies in the inverted baseline FWI model. Indeed, the bandwidth of the data, from a 16 Hz Ricker wavelet, cannot resolve all the short-wavelength structures present in the true baseline model (Figure 2a). Inaccuracies exist in the inverted baseline FWI model. In comparison, time-lapse FWI using the proposed method successfully constrains both short- and long-wavelength perturbations, as shown in Figure 2f, while also achieving a MOR of approximately 17.

Our proposed method employs a non-uniform resolution of the RBF grid, which introduces an implicit form of

regularization. This is achieved by allocating finer RBF centers to the reservoir area and coarser ones to the overburden. Consequently, this allocation strategy inherently provides an implicit regularization effect. Maharramov & Biondi (2016) developed a simultaneous inversion method and introduced an explicit regularization term on model updates to address a similar problem. But choosing proper weights is nontrivial in practice. Additionally, adopting a multi-scale inversion strategy can be another possible solution to constrains both short- and long-wavelength well.

Near-surface monitoring with surface waves

We further extend the proposed method to elastic FWI with surface waves for near-surface monitoring. High-frequency dispersive surface waves propagate at shallow depths, while lower-frequency content propagates to greater depths. As a result, the resolution of the surface wave FWI decreases with depth. RBF allows this varying resolution by distributing the interpolation centers accordingly. Figure 3a shows the targeted monitor S-wave velocity model, with four anomalies overlaid on the background velocity model, which is further detailed in Figure 3c. We choose the position of RBF centers shown in Figure 3b, where the average distance between those RBF centers gradually increases from the top to the bottom of the model from 15 m to 90 m. Figure 3d shows the inverted S-wave velocity using the conventional FD parameterization, whereas Figure 3e presents the inverted model using our proposed RBF scheme. For this surface-wave FWI problem, the recovery of the anomalies is similar. But in the latter result, the deepest anomaly has a flattened top boundary, which can be attributed to imposed smoothness by the interpolation of the RBF. In this case, we achieve an MOR on the order of ~8.

CONCLUSIONS

In this study, we propose using RBF to reparameterize time-lapse FWI problems to reduce the model space. RBF is well-suited to the time-lapse targets as they can adapt to complex structures without the need for uniformly dense grids in the whole computational domain. Through three different synthetic tests, we demonstrate that the proposed RBF-parameterization strategy not only achieves varying degrees of MOR but also maintains the quality of the inverted results. Furthermore, RBFs inherently act as a form of regularization, as evidenced in the second case where both short-wavelength changes in the reflector and long-wavelength changes in the overburden are effectively constrained. We expect that the proposed method will enhance the computational efficiency of inversion methods like the Gauss-Newton and Bayesian approaches by employing a reduced model space.

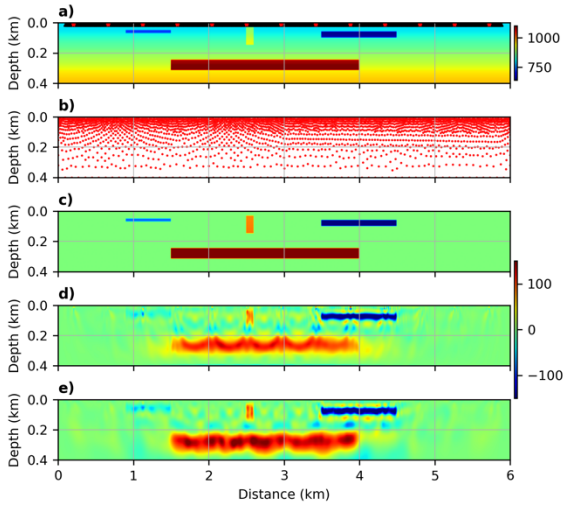

Figure 3: Elastic time-lapse FWI using surface waves for near-surface change monitoring. (a) The monitor S-wave velocity model, where four anomalies are introduced as the time-lapse changes. (b) Strategically positioned RBF centers for reparameterizing the time-lapse changes. (c) True time-lapse changes. (e) Inverted time-lapse changes using conventional FD parameterization. (f) Inverted time-lapse changes using the proposed RBF reparameterization approach. Note: The initial velocity model for inversion is the background S-wave model. The P-wave velocity and density models are obtained by scaling the S-wave velocity model.

ACKNOWLEDGMENTS

We would like to thank Stanford Earth imaging Project (SEP) affiliate companies for financial support. The SEAM model used in this study can be obtained by contacting the SEAM Corporation: https://seg.org/seam.